Treating solar model uncertainties: A consistent statistical analysis of solar neutrino models and data

Evalyn Gates
Department of Astronomy and Astrophysics and Enrico Fermi Institute, The University of Chicago, Chicago, Illinois 60637

Lawrence M. Krauss
Departments of Physics and Astronomy, Case Western Reserve University, Cleveland, Ohio 44106

Martin White
Center for Particle Astrophysics, University of California, Berkeley, California 94720-7304
(Received 27 June 1994)

We describe how to consistently incorporate solar model uncertainties, along with experimental errors and correlations, when analyzing solar neutrino data to derive confidence limits on parameter space for proposed solutions of the solar neutrino problem. Our work resolves ambiguities and inconsistencies in the previous literature. As an application of our methods we calculate the masses and mixing angles allowed by the current data for the proposed MSW solution using both Bayesian and frequentist methods, allowing purely for solar model flux variations, to compare with previous work. We also show that solutions which simply suppress the ^{8}B solar neutrino flux are strongly disfavored and have a likelihood ratio of at most 10^{-8} compared to the best MSW solution. Finally, we consider the effects of including metal diffusion in the solar models and also discuss implications for future experiments.

PACS number(s): 96.60.Kx, 12.15.Ff, 14.60.Pq

I. INTRODUCTION

As more experimental information has become available and theorists have converged on "new-physics" explanations [1–3,5–8] of the solar neutrino problem there has been interest in incorporating the error budget of solar models into analyses of the data. This has proceeded in stages. Solar model flux uncertainties were first incorporated in [4]. The first effort to exploit them in a quantitative comparison with data was [1], which however did not take experimental correlations into account. Recently, a detailed analysis has been performed which has largely resolved this problem by a correct accounting for experimental correlations, as well as a careful examination of such effects as Mikheyev-Smirnov-Wolfenstein (MSW) [9] mixing in the Earth in order to derive allowed regions of mass and mixing angle [10]. Nevertheless, the general applicability of the approximations used there to model solar model uncertainties is not obvious. In addition, the determination of confidence limits and allowed regions of parameter space uses a nonstandard statistical analysis.

Now that it appears that the gallium results are stable and that no new significant experimental light is likely to be shed on the problem until the gallium experiments have been checked with neutrino sources (GALLEX is scheduled for "calibration" in June 1994) or the next generation of detectors comes on line in 3–4 years, there is time to consider a comprehensive, consistent statistical analysis, vis-à-vis neutrino-based solutions of the solar neutrino problem. (Neutrino-, rather than solar-model-, based solutions are now strongly indicated by the present data, even without including the Homestake results [6,8].) Such an analysis is the purpose of the present paper. We shall demonstrate a technique which treats known solar model uncertainties in a computationally simple fashion, and then describe how to incorporate the existing experimental information in order to derive confidence limits on neutrino masses and mixing angles which have a well-defined statistical meaning. In the approximation in which all solar model uncertainties can be parametrized in terms of the neutrino flux uncertainties, this technique yields allowed regions in parameter space which can be compared with previous results.

The determination of allowed regions requires four distinct parts: (1) a calculation of solar model uncertainties, (2) a model of neutrino transport and detection probabilities, (3) a determination of experimental uncertainties and correlations, and finally (4) a well-defined statistical procedure for comparing predictions and observations.

The outline of the paper is as follows. We first describe solar model uncertainties gleaned from Monte Carlo studies of solar models. We demonstrate that the essential information about this type of solar model uncertainty is contained in the neutrino flux correlation matrix, which can be calculated either directly using the solar models themselves, or else using a simple but well-defined approximation. Next we demonstrate how to translate these flux correlations into an experimental covariance matrix necessary to incorporate properly the experimental error budget. Following this we describe, for both MSW and vacuum oscillations, how one derives survival probabilities following transport through the Sun and Earth. Finally, we describe how to consistently derive

allowed regions for neutrino parameter space using well-defined statistical probes in a way which avoids problems with past analyses, and discuss the meaning of our results for future experiments and particle physics models.

It is worth emphasizing in advance that by outlining a well-defined statistical procedure for comparing theory and observation we do not necessarily subscribe to the view that only statistical solar model uncertainties are relevant, or even that they may be the most important uncertainties. It is possible that systematic uncertainties, due to the introduction of new physics into the solar models, could shift the *entire* allowed range of model parameters determined by the methods we describe here. As the standard solar model gets more complete, this will be less likely. As an example we show that the inclusion of new physics in the form of heavy metal diffusion has a noticeable but small effect on the allowed regions. In any case our purpose here is to define a consistent and correct procedure which may be applied as both the data and the theoretical models improve.

II. SOLAR MODEL UNCERTAINTIES

Comprehensive estimates of the present solar model uncertainties have been made by Bahcall and collaborators [11,12], who performed detailed Monte Carlo analyses of the neutrino fluxes that result when solar model input parameters are varied over their allowed ranges. Since calculating many full solar models can prove cumbersome in terms of computing time, it is useful to have a reliable and efficient approximation scheme which reproduces the results of such a calculation. Several schemes have been proposed which account for the variation in the total flux of neutrinos, which is in general the major source of uncertainty (from solar physics) in the prediction of the experimental rates.

Two different approaches have been applied to this problem. The first involves simplifying the solar model parameter space, an example of which we will call "the T_c approach" [13]. Here the fluxes are parametrized by a single (solar model *output*) variable—the core temperature of the sun, T_c. The temperature dependence of the various fluxes are derived from the scatter plots of flux vs T_c from solar-model Monte Carlo calculations. (See, e.g., Figs. 6.2 and 6.3 in Ref. [12].) Approximating the temperature dependence of the fluxes by power laws in T_c specifies the flux distributions, with the error in T_c determined so as to give the appropriate uncertainties in the fluxes.

While the scatter plots indicate that the relationship between the neutrino flux and T_c can be approximately described by a simple power law, this relationship is only approximate, and there remains a significant width to the straight line that would describe a perfect power-law dependence. Because of this width, these plots do not indicate how the various fluxes are correlated. For example, a solar model with a high T_c may correspond to an increased *pp* flux, but little or no corresponding decrease in the ^{8}B flux. The T_c method, based on only *one* parameter, of course produces totally (anti)correlated uncertainties for the neutrino fluxes while the solar model flux uncertainties exhibit a wide range of correlations. The differences in the correlations for the T_c parametrization and the full solar-model Monte Carlo calculation are a reflection of the scatter in the plots of [12]. By overestimating the correlations, the T_c approach tends to underestimate the size of the allowed parameter region for a given confidence level. We note also that the T_c method fails completely for the "maximum rate model" of Bahcall and Pinsonneault [16]. Thus while a T_c parametrization can be a useful tool in some instances, and gives physical insight into the basic mechanism of the flux distributions, it is not appropriate for calculating solar model uncertainties [2]. We note that above we have discussed the simplest application of the T_c "model," and these criticisms are not meant to apply to [13]. The relevance of extra degrees of freedom beyond T_c was noted in [13], who included the effect of nuclear cross section uncertainties. Unfortunately a detailed examination of their results is not possible since there is no specification of how this was done.

An updated version of this method [10] includes not only T_c but also cross section uncertainties in the form of two extra parameters, chosen from among the (nuclear cross section) input parameters to the solar models. This allows this method to be tuned to approximate more closely the full solar model correlations [10]. Any method which reproduces the flux correlation matrix can correctly include the solar model errors, so this updated method and the "power-law method" (described below) should agree on the statistical content of the solar model uncertainty. However, the applicability of this method, including the determination of which combination works, and which T_c uncertainty to use can only strictly be determined after the fact by explicitly utilizing the detailed results of the full solar-model Monte Carlo calculations.

An alternative approach, proposed earlier [1], parametrizes the solar model uncertainties in terms of the logarithmic derivatives of the fluxes with respect to the 10 solar-model *input* parameters. It was shown in [12] that for reasonable variations in the input parameters the neutrino fluxes ϕ can be expressed as

$$\phi_j \propto \prod_k (\Gamma_k)^{\alpha_{j,k}} \tag{1}$$

where $\alpha_{j,k}$ is the logarithmic partial derivative of ϕ_j ($j = pp, \mathrm{pep}, \mathrm{hep}, {}^7\mathrm{Be}, {}^8\mathrm{B}, {}^{13}\mathrm{N}, {}^{15}\mathrm{O}$, and $^{17}\mathrm{F}$) with respect to the input parameter Γ_k. The solar model flux uncertainties can thereafter be obtained from a Monte Carlo procedure assuming Gaussian distributions for the input parameters, as described in more detail in [1]. This method has a firm basis in describing the errors in the output function (solar model fluxes) in terms of the errors in the input parameters, and the $\alpha_{j,k}$ are readily available [12]. We shall refer to this as "the power-law approach."

From a Monte Carlo analysis using this approach, we obtain an estimate of the theoretical uncertainties in the predicted fluxes for each species. This allows us to determine the correlations between the various fluxes, which will be important for computing correlations between the

TABLE I. The experiment and flux correlations (×100) computed using the 1000 solar models of Bahcall and Ulrich.

	H	K	Ga	pp	pep	hep	^{7}Be	^{8}B	^{13}N	^{15}O	^{17}F
H	100	99	97	-	-	-	-	-	-	-	-
K	99	100	95	-	-	-	-	-	-	-	-
Ga	97	95	100	-	-	-	-	-	-	-	-
pp	-	-	-	100	77	16	−91	−72	−88	−88	−88
pep	-	-	-	77	100	28	−69	−50	−73	−71	−72
hep	-	-	-	16	28	100	5	−15	−46	−45	−45
^{7}Be	-	-	-	−91	−69	5	100	74	80	80	80
^{8}B	-	-	-	−72	−50	−15	74	100	73	73	73
^{13}N	-	-	-	−88	−73	−46	80	73	100	99	99
^{15}O	-	-	-	−88	−71	−45	80	73	99	100	99
^{17}F	-	-	-	−88	−72	−45	80	73	99	99	100

rates predicted for different detectors. The elements of the covariance matrix for the various fluxes (ϕ_j) are given by [14]

$$V_{jk} = \langle (\phi_j - \bar{\phi}_j)(\phi_k - \bar{\phi}_k) \rangle \tag{2}$$

where the angular brackets indicate an average over the solar models and $\bar{\phi} = \langle \phi \rangle$. To display the correlations we present the correlation matrix, whose elements are given by

$$\rho_{jk} = \frac{V_{jk}}{\sigma_j \sigma_k}, \tag{3}$$

where $\sigma_j = \sqrt{V_{jj}}$ is the standard deviation in ϕ_j. Note that in the correlation matrix the diagonal elements are 1 by definition and off-diagonal elements are equal to (−)1 in the limit of perfect (anti)correlation.

It is important to note that the partial derivatives in (1) were determined via the solar model with fixed solar luminosity. Even though the power law approach does not explicitly enforce such a constraint, the use of the relation (1) will result in a covariance matrix equal to that from the fully self-consistent solar-model Monte Carlo calculations. This was implicitly exploited in our previous work [1,15] and is explicitly demonstrated in Tables I and II which compare the covariance matrices for the two approaches. The agreement between our Monte Carlo calculation and the 1000 models of Bahcall and Ulrich is good, as one would expect, except for the hep neutrinos. Since the hep and ^{17}F contribute negligibly to the rate in all the detectors this is not of concern. The flux correlation matrix for the T_c approach has all elements equal to ±1 since there is perfect correlation—i.e., all the fluxes depend on one parameter. This is relaxed in the updated approach including the cross section uncertainties [10] which it is claimed also reproduces Table I.

As we shall discuss later, at least as far as flux uncertainties are concerned, the relevant statistical content of the full solar-model Monte Carlo calculation is contained in the covariance matrix V_{ij}. Our method is designed to reproduce this matrix based on the matrix of flux derivatives, while the updated T_c approach reproduces this matrix by *a posteriori* construction. Nevertheless, once the matrix V_{ij} is obtained from the solar models, this alone is sufficient, and there is no need for either approximation. For this reason, this quantity is as important to extract from solar model calculations as are logarithmic flux derivatives $\alpha_{j,k}$, and we suggest that future work on solar model calculations include the results for V_{ij} explicitly.

In our fits, to be described later, we use the updated fluxes from the Bahcall and Pinsonneault solar model [16] which incorporates Helium diffusion and new equation of state and opacity calculations. Although a full Monte Carlo treatment of the flux uncertainties has not been performed for this model we have updated the correlation matrix shown in Table II to incorporate the errors on the input parameters as given in [16]. This does not include the uncertainty in the fluxes from variations in diffusion, but is the best use of currently available information.

III. EXPERIMENTAL RATE UNCERTAINTIES

The central quantity to use in determining how well model predictions agree with the observed rates will be the rate covariance matrix. When solar model uncertainties can be completely parametrized in terms of the flux covariance matrix, the covariance matrix for the rates can be calculated directly from that for the fluxes. In this case, for any theoretical model the predicted rate in

TABLE II. The experiment and flux correlations (×100) computed using the power-law Monte Carlo approach.

	H	K	Ga	pp	pep	hep	^{7}Be	^{8}B	^{13}N	^{15}O	^{17}F
H	100	99	95	-	-	-	-	-	-	-	-
K	99	100	92	-	-	-	-	-	-	-	-
Ga	95	92	100	-	-	-	-	-	-	-	-
pp	-	-	-	100	77	8	−90	−74	−88	−88	−88
pep	-	-	-	77	100	12	−70	−53	−71	−69	−71
hep	-	-	-	8	12	100	2	−6	−21	−20	−21
^{7}Be	-	-	-	−90	−70	2	100	75	77	77	80
^{8}B	-	-	-	−74	−53	−6	75	100	73	73	75
^{13}N	-	-	-	−88	−71	−21	77	73	100	100	97
^{15}O	-	-	-	−88	−69	−20	77	73	100	100	96
^{17}F	-	-	-	−88	−71	−21	80	75	97	96	100

the detector R_a ($a = \mathrm{H, K, Ga}$) is a linear combination of the fluxes ϕ_j with coefficients functions of the theory parameters [see Eq. (23)]. If we write $R_a = r_{aj}\phi_j$ with $r_{aj} = r_{aj}(\Delta m^2, \sin^2 2\theta)$ then it is straightforward to show that

$$V_{ab} = \sum_{jk} r_{aj} r_{bk} V_{jk} \ . \tag{4}$$

It is important to note that at this stage experimental uncertainties, including those from detection cross section uncertainties have not been introduced.

The correlation matrices for both the fluxes and the experiments (assuming standard model interactions for the neutrinos) are shown in Tables I and II for the Bahcall and Ulrich standard solar model(s) [11] and our power-law approach. Note that the experimental rates are almost perfectly correlated (a fact which was ignored in our earlier work [1]). The correlation between experiments can decrease once neutrino mixing is allowed. For example the correlations can be as low as $\sim 25\%$ for $(\Delta m^2, \sin^2 2\theta)$ in the small-angle allowed region (see Fig. 2), however generally the correlation is above 80%. It is initially surprising that the rates for Homestake and Kamiokande, which measure principally ^{8}B neutrinos, should be (strongly) *positively* correlated with gallium, which measures principally *pp* neutrinos, when ^{8}B and *pp* neutrinos are strongly *anticorrelated!* The resolution of this apparent paradox is that while the major contribution to the gallium *rate* is due to *pp* neutrinos, the ^{8}B and ^{7}Be neutrino fluxes are much more uncertain and are the principal contribution to the *uncertainty* in the gallium rate. For gallium

$$R_{\mathrm{Ga}} = 71pp + 34{}^7\mathrm{Be} + 14{}^8\mathrm{B} + \cdots \ \mathrm{SNU(solar\ neutrino\ units)}. \tag{5}$$

The relative errors of the *pp*, ^{7}Be, and ^{8}B fluxes are $\frac{1}{2}\%$, 5%, and 15%, respectively. Clearly the uncertainty in ^{7}Be and ^{8}B dominates the solar model induced uncertainty in the gallium rate. (Note once again that at this stage detector cross section uncertainties have not yet been introduced.)

IV. NEUTRINO TRANSPORT

In order to determine the experimental rate matrix described above, we must utilize analytic or numerical techniques to propagate neutrinos through the Sun, empty space, and the Earth in order to determine survival probabilities and resulting flux modulations. The methods used differ, depending upon whether one is interested in the region of mass and mixing angle space where MSW oscillations or vacuum oscillations are important.

A. Vacuum oscillations

In addition to the MSW model, there exists the possibility that the observed deficit of neutrinos could be due to oscillations in vacua between the Sun and the Earth [17]. In this case the details of the production in the sun are unimportant, and we need keep track only of total flux variations. The survival probability is [12]

$$P(\nu_e \to \nu_e) = 1 - \sin^2 2\theta \sin^2 \frac{\pi L}{L_V} \tag{6}$$

with $L_V = 4\pi E/\Delta m^2$. Additionally one can average this survival probability over the change in the Earth-Sun distance during times comparable with the average duration of an experimental "run." We find our conclusions do not depend on the averaging.

Performing a fit to the current experimental data (as described later) we find a small region in parameter space which is allowed at the 95% confidence level. This region agrees in general with those found by other authors [19,18], who have explored this theory in detail, and we will have nothing further to say about it.

B. MSW oscillations

Perhaps the most promising neutrino mixing solution to the solar neutrino problem is the Mikheyev-Smirnov-Wolfenstein (MSW), or matter-enhanced mixing, model [9,12]. In this section we give details of our approximations and modeling of this effect in relation to computing the predicted rates in the Homestake [20], Kamiokande [21], and gallium [22,23] neutrino experiments.

To compute the rate predicted by a model for any detector we need information about the neutrino production in the Sun. We use the flux distributions over the production regions $d\phi_i(r)$ and the electron number density as a function of solar radius, $N_e(r)$, from [12] and the scale heights at resonance r_0 tabulated in [24] for use with their analytic approximations.[1] We have explicitly checked that using $r_0 \equiv N_e^{\mathrm{res}}/|dN_e/dr|_{\mathrm{res}}$ from the Bahcall and Pinsonneault standard solar model [16] produces the same results. Additionally we assume that the energy spectrum of neutrinos at each r is as described in [12]. We have fitted the spectra for all species as a polynomial times the relevant β-decay spectrum (correcting the typographical error in Eq. 8.15 of [12]). These values are then input into the analytic expressions for the ν_e survival probability [24] (see also [25]), as outlined in our previous work [15] and summarized below.

If the neutrino passes through a resonance on its way through the Sun then we define

$$4n_0 = r_0 \left(\frac{\Delta m^2}{2E}\right)\left(\frac{\sin^2 2\theta}{\cos 2\theta}\right) , \tag{7}$$

where $N_e(r)$ is the electron density profile in the Sun. The electron density at resonance is given by

[1] We correct a programming error in our earlier work in which r_0 was incorrectly read from the table.

$$N_e^{\rm res} = \left(\frac{\Delta m^2}{2E}\right)\left(\frac{\cos 2\theta}{\sqrt{2}G_F}\right). \quad (8)$$

In terms of n_0 we classify the transition as either adiabatic ($4n_0 \gg 1$) or nonadiabatic ($4n_0 \leq 1$).

Let $N_e^{(0)}$ be the electron density at the point of ν production, then for neutrinos in the adiabatic region, or those in the nonadiabatic region with $N_e^{\rm res} < N_e^{(0)}/(1+\tan 2\theta)$ the analytic expression for the ν_e survival probability is given by [24]

$$P(\nu_e \to \nu_e) = \frac{1}{2} + \left(\frac{1+e^{-x}}{1-e^{-x}}\right)\left[\frac{1}{2} - \frac{e^{-y}}{1+e^{-x}}\right] \times \cos 2\theta_m \cos 2\theta, \quad (9)$$

where

$$x = 2\pi r_0 \frac{\Delta m^2}{2E}, \quad (10)$$

$$y = 2\pi n_0 (1 - \tan^2\theta), \quad (11)$$

$$\cos 2\theta_m = (1-\eta)/\sqrt{(1-n)^2 + \tan^2 2\theta}, \quad (12)$$

$$\eta \equiv N_e^{(0)}/N_e^{\rm res}. \quad (13)$$

For neutrinos in the nonadiabatic region produced near resonance, $N_e^{(0)}/(1+\tan 2\theta) \leq N_e^{\rm res} \leq N_e^{(0)}/(1-\tan 2\theta)$, the corresponding expression for the survival probability is

$$P(\nu_e \to \nu_e) = \frac{1}{2}[1 + \exp(-\pi n_0)], \quad (14)$$

while for nonadiabatic transitions with $N_e^{\rm res} > N_e^{(0)}/(1-\tan 2\theta)$ or adiabatic transitions with $N_e^{\rm res} > N_e^{(0)}$ we use

$$P(\nu_e \to \nu_e) = \frac{1}{2} + \frac{1}{2}\cos 2\theta_m \cos 2\theta. \quad (15)$$

We have also included in our analysis the effects of double resonances in the Sun, see [15].

C. Earth effects

It has long been known [26] that for Δm^2 near 10^{-6} eV^2 and large $\sin^2 2\theta$ it is possible to "regenerate" ν_e by having neutrinos pass through the Earth. The survival probability $P(\nu_e \to \nu_e)$ is very sensitive to the path length of the neutrinos in the Earth, and so neutrinos with parameters in this range should give rise to day-night and seasonal variations in the observed flux. Since no such effect has been seen [21] this serves to rule out a region of parameter space near $\Delta m^2 \sim 10^{-6}$ eV^2 and $\sin^2 2\theta \sim 0.2$.

We follow [27] in including this "Earth effect" in our fits, though our treatment differs from theirs. Rather than keep track of the predicted dependence of $P(\nu_e \to \nu_e)$ on the path length (which changes during the "night") and fit to the data in many bins[2] we choose to use a number which summarizes that no effect is actually seen. (This makes our result less sensitive to the detailed statistics of the full day-night data. In any case, as we later display, incorporating day-night effects has a minimal effect at present on the allowed regions.) Consequently we use the quoted measurement of [21]

TABLE III. The model Earth that we used in calculating the regeneration effect. Densities in column 2 are given in g/cm^3 and the final column is in 10^{-7} eV^2/MeV, assuming $n_p = n_n$ for the Earth interior.

$R/R_\oplus$	ρ	$\langle\sqrt{2}G_F N_e\rangle$
0.0000–0.1910	12.858	4.87
0.1910–0.5471	11.024	4.18
0.5471–0.8948	4.964	1.88
0.8948–0.9341	3.923	1.49
0.9341–1.0000	2.292	0.87

$$\left\langle \frac{\text{day} - \text{night}}{\text{day} + \text{night}} \right\rangle\Bigg|_{\rm year} = -0.08 \pm 0.11 \quad (16)$$

which is independent of the solar model flux uncertainties. (This was obtained for thresholds of both 7.5 MeV and 9.3 MeV as the experiment lowered its threshold. Since there was no evidence of an effect at either threshold we use the lower, i.e., 7.5 MeV in our analysis.) Since this quantity does not depend on the neutrino flux we simply add the χ^2 from this fit to the χ^2 obtained from fitting to the time average rates as will be described later. (Correlations between the two measures will not be expected to alter substantively our results since the data shows no evidence for variations in any case.) The effect will be to rule out a region of parameter space where a large day-night effect would be predicted.

To predict the left-hand side (LHS) of (16) we follow [27,28]. Since only the integrated electron density along the line of sight matters for the average $P(\nu_e \to \nu_e)$ we model the Earth as five concentric shells of constant electron density N_e, which we have taken from the models of [29] and listed in Table III. Including the Earth effect the survival probability of a ν_e which has MSW survival probability $P_{\rm MSW}$ is given by [27,28]

$$P_E = P_{\rm MSW}|a|^2 + (1 - P_{\rm MSW})|b|^2 + \left(\frac{1}{2} - P_{\rm MSW}\right)\tan 2\theta (ab^* + ba^*) \quad (17)$$

where a and b are elements of the unitary matrix which

[2]We note in passing that the binned data of [21] for the day-night effect has a very low χ^2 per degree of freedom, which may indicate correlated (systematic) uncertainties in this data set. While it is not impossible that data with such small scatter could arise as a statistical fluctuation, in any case such a low χ^2 will bias a fit in which these points form most of the degrees of freedom. This is one reason why we utilize the method described above.

describes the evolution of neutrinos through the Earth:

$$\begin{pmatrix} \nu_e(t) \\ \nu_x(t) \end{pmatrix} = \begin{pmatrix} a & b \\ -b^* & a^* \end{pmatrix} \begin{pmatrix} \nu_e(0) \\ \nu_x(0) \end{pmatrix} . \tag{18}$$

Once we have solved for this matrix for an arbitrary shell of our model Earth we can obtain the full matrix by multiplication of the evolution matrices for each shell in the appropriate order (entering and leaving). Thus the problem reduces to calculating a and b for propagation through a shell of constant N_e. Dropping a constant energy offset from ν_e and ν_x, which contributes only an irrelevant overall phase, the evolution equation is

$$i\frac{d}{dt}\begin{pmatrix} \nu_e \\ \nu_x \end{pmatrix} = \left[\left(\frac{G_F N_e}{\sqrt{2}} - \frac{\Delta m^2}{4E}\cos 2\theta\right)\sigma_3 + \frac{\Delta m^2}{4E}\sin 2\theta\ \sigma_1\right]\begin{pmatrix} \nu_e \\ \nu_x \end{pmatrix} \tag{19}$$

where σ_i are the Pauli matrices. We solve this using the identity $\exp[i\vec{a}\cdot\vec{\sigma}] = \cos|a|\mathbf{1} + i\sin|a|(\hat{a}\cdot\vec{\sigma})$ to yield

$$a = \cos|h| - i\hat{h}_3\sin|h| ,$$
$$b = -i\hat{h}_1\sin|h|, \tag{20}$$

with

$$\vec{h} = \left(\frac{\Delta m^2}{4E}\sin 2\theta,\ 0, \frac{G_F N_e}{\sqrt{2}} - \frac{\Delta m^2}{4E}\cos 2\theta\right) \times \text{path length} \tag{21}$$

and $\hat{h} = \vec{h}/|h|$. Although our model is relatively crude, given that we are trying to fit to the absence of an effect it is sufficient for our purposes.

The final task is then to integrate over the paths through the Earth during the course of the night-year. In our model Earth with spherical symmetry the path is totally defined by giving the angle θ_0 subtended at the center of the Earth by the point of entry of the ν beam and the detector. In the limit that the Earth-Sun distance is much larger than the Earth's radius we have that

$$\cos\left(\frac{\pi - \theta_0}{2}\right) = \sin\delta\sin i + \cos\delta\cos i\cos(\phi + \pi) \tag{22}$$

where ϕ is the azimuthal angle between the Sun and the detector as measured from the center of the Earth, δ is the detector latitude, and $i = 23°.5\sin(\omega_\odot t)$ is the inclination of the ecliptic to the Earth's equator. Averaging over ϕ and $\omega_\odot t$ we obtain the distributions for θ_0, with which we can then determine the ν_e survival probability averaged over night-year. For a given mass and mixing angle, we compare this value with the RHS of (16) in determining the χ^2 fit to the data. The survival probability $P(\nu_e \to \nu_e)$ including the Earth effect is shown in Fig. 1 for a parameter set which can be compared with Fig. 3(b) of [28].

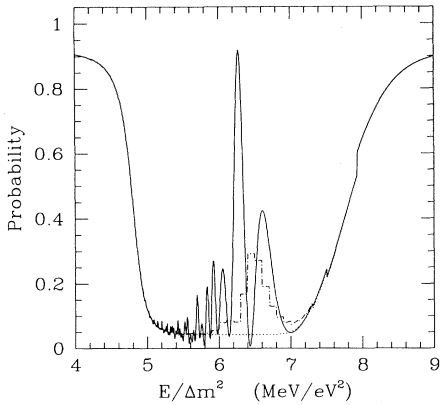

FIG. 1. The survival probability $P(\nu_e \to \nu_e)$ including the Earth effect for mixing angle $\sin 2\theta = 0.4$. The dotted line is the MSW probability without the Earth effect, the solid line is the probability for a neutrino passing through the center of the Earth, and the dot-dashed line shows the probability averaged over the night-year.

D. Calculating the rates

Using the above and the formulas for $P_{\rm MSW}$ outlined in the previous section we computed the survival probability averaged over the night and the year. These probabilities and the fluxes for each species, j, are then convolved with the detector response $D_i(E_\nu)$ [1,12,15,30,31] for neutrinos of flavor i and energy E_ν to get the predicted rate

$$R = \sum_{ij}\int dE_\nu \phi_j(E_\nu) P_i(E_\nu) D_i(E_\nu) \tag{23}$$

for each model. We include the contributions from $j = pp(10)$, pep(1), ^{7}Be(2), ^{8}B(30), ^{13}N(20), and ^{15}O(20) neutrinos, where the number in parentheses after each species is the number of energies computed for each spectrum in the integration. The contribution from hep and ^{17}F neutrinos are less than 1/2% for all the experiments and can be safely ignored. Our results for the iso-SNU contours for the Homestake, Kamiokande, and Gallium experiments compare well with those in [10].

V. DATA AND MODEL TESTING

We use the latest data for the time-averaged rate in the Homestake [20], Kamiokande [21], SAGE [22], and GALLEX [23] experiments. Since the theory predictions for the SAGE and GALLEX experiments are identical and the experimental values agree within errors, we have combined the two rates (74 ± 20 and 79 ± 12 SNU for SAGE and GALLEX, respectively) in our fit. We have added the statistical and systematic errors in quadrature, since they are independent. The assumption of a Gaussian distribution for the systematic error is problematic because, by its very nature, the systematic error has no statistical distribution. However, if we regard the Gaussian as representing the state of our knowledge

about the systematic error then clearly a function which penalizes large "errors" is more appropriate than a flat distribution (which would correspond to maximal ignorance of the size of the systematic error). We have chosen a Gaussian for simplicity. The three experimental rates, as a fraction of the standard solar model predictions, are shown in Table IV. In our analysis we have added the cross section uncertainties [11] in quadrature to the quoted errors. For gallium this ignores the energy dependence of the uncertainty from the resonance, but this uncertainty affects primarily the ^{8}B contribution to the rate which is already small and which we expect to be suppressed for the masses and mixing angles of interest to us.

We have used two parametric methods: a χ^2 goodness-of-fit procedure and a Bayesian likelihood analysis [14] to compare the measured rates $R_a^m \pm \sigma_a$ (a=H,K,Ga) to the rates predicted by the model $(\Delta m^2, \sin^2 2\theta)$. Both methods rely on the assumption that the errors in the solar model predictions are Gaussian under small variations in the solar model input parameters, which appears to be a good assumption [12]. For more discussion of the methods we use see [14,32–34].

Including the solar model uncertainties, each set of MSW parameters $(\Delta m^2, \sin^2 2\theta)$ defines a distribution of rate triplets R_a. One can calculate the covariance matrix $V_{ab}^{\rm SM}$ for the triplets analogously to Eqs. (2) and (4). To the theoretical solar model covariance, $V_{ab}^{\rm SM}$, we add the experimental errors, σ_a (when the quoted errors are asymmetric we add upper and lower intervals in quadrature to obtain σ_a), to obtain the full covariance matrix: $V_{ab} = V_{ab}^{\rm SM} + \sigma_a^2 \delta_{ab}$. Defining [14]

$$\chi^2 \equiv (R_a - \bar{R}_a) V_{ab}^{-1} (R_b - \bar{R}_b) \ , \qquad (24)$$

where $\bar{R}$ is the standard solar + neutrino-mixing model rate prediction, the distribution of χ^2's defined by the theory is a χ^2 distribution with 3 degrees of freedom (or 4 degrees of freedom if we include the day-night measurement). The statement that the theory is ruled out at some confidence level is the claim that the χ^2 for the measured triplet (quartet) lies in the large-χ^2 tail of the distribution defined by the theory, i.e., that the measured value is unlikely. If the *data* are within the 95% confidence level of a given theory we say the *theory* parameters are allowed at the 95% confidence level by the data.

Previous authors have generally implemented instead a *best-fit* procedure that attempts to estimate the parameters Δm^2 and $\sin^2 2\theta$ from the data and assign errors to the inferred values. One takes the parameters which minimize χ^2 as the central values, with an *allowed range* given by the condition that $\chi^2(\Delta m^2, \sin^2 2\theta) < \chi^2_{\rm min} + \nu$, with ν determined by the range of σ desired and the number of parameters being estimated. Such an approach is based on the maximum likelihood procedure under the assumption that the correlation matrix is independent of the parameters being estimated. (This assumption is obviously not true for this case, but the errors introduced turn out to be numerically small.) This approach makes the additional assumption that $\chi^2(\Delta m^2, \sin^2 2\theta)$ is well approximated by a quadratic over the relevant range of parameters. As can be seen in Fig. 2 this assumption is clearly false over the range of $(\Delta m^2, \sin^2 2\theta)$ of interest. It is important to realize that the statistical answers one gets depend upon the questions one asks. This method *does not* address the question of what regions of model space are allowed by the data, but rather what regions provide a best fit under the assumption that the model is correct, for *some* set of parameters. The allowed region determined differs from that for the method outlined above as it asks a different statistical question: not what models are allowed by the data but what are the errors on the best-fit Δm^2 and $\sin^2 2\theta$.

In addition, an approach for calculating allowed regions has recently been advocated [10] which uses nonstandard definition of χ^2. In comparing their method to solar-model Monte Carlo calculations [11] the authors define "χ^2" in terms of the logarithm of the "average probability" rather than computing V_{ab} for the Bahcall and Ulrich solar models directly and using Eq. (24). The distribution of this χ^2 will not be χ^2, and will not take into account correlations in the rates in a well-defined way. To use consistently such a statistic, the correct distribution and confidence levels to be associated with it would need to be calculated.

An alternative method, which is similar in spirit to the best-fit approach, is to calculate the 2D likelihood func-

TABLE IV. The experimental rates, normalized to the standard solar model predictions, used in the fits. The rates for SAGE and GALLEX have been combined and cross section uncertainties for Homestake and Gallium have been added, in quadrature, to the experimental errors.

Experiment	Rate
Homestake	0.32 ± 0.03
Kamiokande	0.51 ± 0.07
Gallium	0.59 ± 0.08

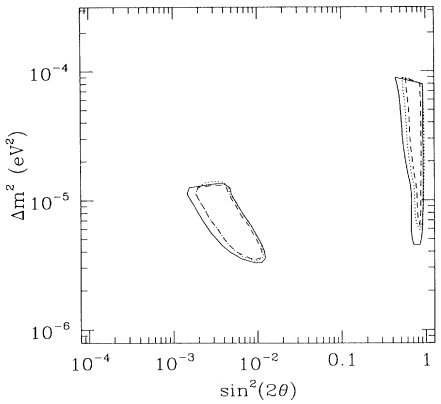

FIG. 2. Region of MSW mass-mixing angle space allowed at the 95% confidence level for the combined Homestake-Kamiokande-Gallium data including solar model uncertainties from the χ^2 analysis (solid). Also plotted is the 95% confidence region from the likelihood function analysis (dotted) and the region obtained by requiring $\chi^2 < \chi^2_{\rm min} + \nu$ (dashed).

tion $\mathcal{L}(\Delta m^2, \sin^2 2\theta)$, again under the assumption that the variations in model predictions (and the experimental errors) are Gaussian. In this case the likelihood function is defined as[3]

$$\mathcal{L} \propto \frac{1}{\sqrt{\det V}} \exp\left[-\frac{1}{2}\chi^2\right] \tag{25}$$

By use of Bayes' theorem, the conditional probability for Δm^2 and $\sin^2 2\theta$, given the experimental measurements, is proportional to the likelihood function times the *a priori* probability distribution for the MSW parameters [33] (for an alternative interpretation see [34]), which is usually referred to as the posterior distribution. If we assume, from scaling arguments, that logarithmic intervals in Δm^2 and $\sin^2 2\theta$ are equally likely, before any experiment is performed, then the posterior distribution is simple proportional to the likelihood function $\mathcal{L}(\log \Delta m^2, \log \sin^2 2\theta)$.

To calculate the 95% confidence regions for Δm^2 and $\sin^2 2\theta$ we follow the method used in assigning regions for Gaussian distributions (which $\mathcal{L}$ is not). Let us define a region in parameter space

$$A(\lambda) \equiv \{(\log \Delta m^2, \log \sin^2 2\theta) | \mathcal{L}(\log \Delta m^2, \log \sin^2 2\theta) > \lambda\}. \tag{26}$$

Then

$$\Gamma(\lambda) \equiv \int_{A(\lambda)} \mathcal{L}(\log \Delta m^2, \log \sin^2 2\theta) d(\log \Delta m^2) d(\log \sin^2 2\theta) \tag{27}$$

is a continuous, monotonic decreasing function of λ, and the 95% confidence region is given by $A(\lambda_*)$, where $\Gamma(\lambda_*) = 0.95\Gamma(0)$. (We note that this method is somewhat arbitrary for multiply peaked likelihood functions such as ours, but it is nonetheless well defined.) This confidence region is interpreted as the region that contains, with 95% probability, the true values of Δm^2 and $\sin^2 2\theta$. Although the interpretation of the region is different than that allowed by the χ^2 method, the two regions are encouragingly similar. In the limit that the likelihood function were Gaussian (χ^2 is a quadratic function of Δm^2 and $\sin^2 2\theta$ and det V is constant) the regions would be ellipses as in [10]. Thus the departure from elliptical shape is an indication that the likelihood function (see Fig. 3) is not simply Gaussian.

[3]Note that the authors of [10] define a likelihood function as a sum of Gaussians and redefine ν above to give regions consistent with this approximate likelihood function. While the statistical meaning of this hybrid method is not immediately clear, the final regions obtained are not much different than provided by more conventional statistical treatments.

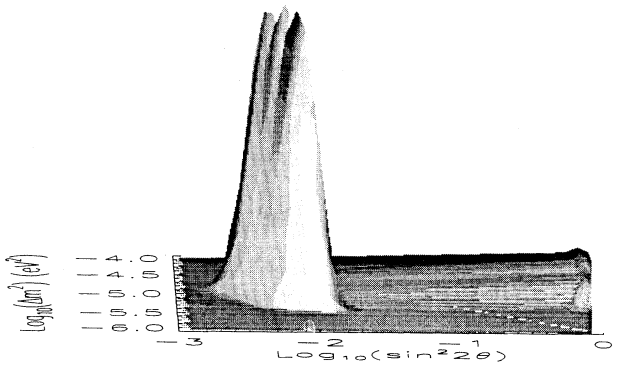

FIG. 3. Likelihood function $\mathcal{L}(\log \Delta m^2, \log \sin^2 2\theta)$ for the combined Homestake-Kamiokande-Gallium data.

VI. RESULTS

Our principal result, the 95% C.L. allowed regions in MSW parameter space, based only on statistical uncertainties in the present formulation of the standard solar model, is shown in Fig. 2 for both the χ^2 and $\mathcal{L}$ methods. The regions shown are obtained by requiring that $\chi^2 < 9.49$ (four DOF, for the three experimental rates and the day-night measurement), including both the rate and the day-night fits. We also show the region obtained by requiring $\chi^2 < \chi^2_{\min} + 6.0$ (2 parameters, $\Delta m^2, \sin^2 2\theta$) for comparison.

We see that there are two allowed regions, a large mixing angle (adiabatic) region and a small mixing angle (nonadiabatic) region. The small mixing angle region is favored over the large mixing angle region, though both are "allowed" at the 95% confidence level. Using the likelihood function we can ask what are the relative probabilities of the large and small angle regions, e.g., we find $P(\sin^2 2\theta > 0.1) \simeq 0.3 P(\sin^2 2\theta < 0.1)$ (see [10] for a different way to ask this question).

We also performed a fit of the data to the Bahcall and Pinsonneault standard solar model (BPSSM) [16], and to "models" where the ^{8}B flux is a free parameter ("no new physics" solutions). The likelihood function for the latter set has a maximum at 0.28 of the BPSSM ^{8}B flux. The corresponding χ^2 for this value is 37 (four DOF), while the χ^2 for the BPSSM is 59 (four DOF). Both models thus provide extremely poor fits to the data, the best fitting low-^{8}B model being $\sim 10^{-8}$ times less likely than the best fitting MSW solution!

One of the largest uncertainties in calculating the expected rates comes from $S_{1,7}$, the nuclear cross section parameter for the reaction $^7\mathrm{Be}(p,\gamma)^8\mathrm{B}$. This uncertainty directly affects the flux of ^{8}B neutrinos, and is due to both experimental uncertainties and the difficulty of extrapolating the experimental results to the low energies relevant in the solar interior. There is a significant difference between the cross sections inferred from the two experiments which have been performed at the lowest energies, indicating some significant systematic error in this parameter. The authors of Ref. [16] use a value for

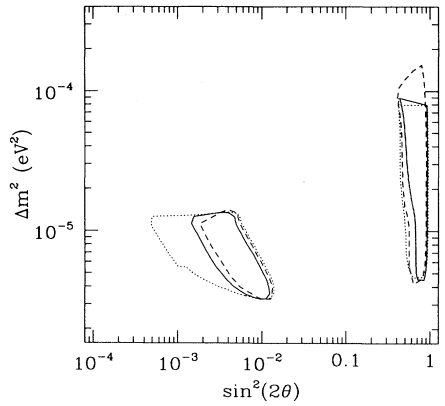

FIG. 4. Region of MSW mass-mixing angle space allowed at the 95% confidence level in the Bahcall and Pinsonneault standard model for the combined Homestake-Kamiokande-Gallium data including normal solar model uncertainties for $\chi^2 < 9.49$ (solid). Also plotted is the 95% confidence region increasing the error on $S_{1,7}$ to 21% (dotted) and the region obtained for fluxes approximating the effects of metal diffusion (dashed, see text).

$S_{1,7}$ that is intermediate to these two results, with errors which do not overlap the central values. This value and its errors, which we have used in determining the correlation matrix, *may* not properly reflect the uncertainty in $S_{1,7}$. In order to explore the implications of a larger estimate for the error in $S_{1,7}$ in Fig. 4 we present the allowed regions assuming as the error for $S_{1,7}$ the difference between the two central values of Refs. [35,36], which corresponds to a 21% uncertainty. As is expected the allowed regions are correspondingly increased.

Recent refinements in solar models, i.e., including heavy element diffusion, have changed the predicted neutrinos fluxes from those of the Bahcall and Pinsonneault model. As we have indicated, changes such as this, which includes new physics rather than new numerical values for the input parameters and their errors, can have a large effect on the allowed regions. The situation with respect to these new solar models is still not settled, and the correlation matrix including parameters for the effects of heavy element and helium diffusion are not yet available. Nevertheless, to estimate the magnitude of the effect of such changes we have used a hybrid procedure which uses neutrino fluxes including heavy element and helium diffusion from [37,38], but our old correlation matrix. Specifically we have artificially changed the fluxes of the Bahcall and Pinsonneault model by percentages equal to those shown in Table V but used the flux correlation matrix from Table II. While this method is not fully consistent, and the fluxes used are preliminary, it should approximate the main effects of these changes and illustrate the possible shift in the allowed regions that can be expected for such models.

We display in Fig. 4 our result for the allowed range of parameter space in this case. The change in the allowed region reinforces our earlier remarks: the potential

TABLE V. The percentage change in the fluxes for each neutrino species in the Proffitt solar model arising from including heavy element diffusion.

Flux	% Change
pp	1 ↓
pep	2 ↓
hep	2 ↓
^{7}Be	5 ↑
^{8}B	14 ↑
^{13}N	4 ↑
^{15}O	24 ↑

change in the allowed regions due to such modifications of the solar model can be larger than indicated by the inclusion of the usual solar model uncertainties. Thus it is prudent to realize that the presently allowed regions are now only suggestive. Further solar model improvements could change their shape, and position, although we do not expect such changes to be large.

VII. FUTURE EXPERIMENTS

At very large mixing angles we expect that the ν_e survival probability will be roughly independent of energy so that the spectrum of neutrinos seen would be unchanged but for the normalization. In the adiabatic region the existence of a resonance implies a large suppression of the ν_e survival probability while the converse is true in the nonadiabatic region [12]. Hence we expect that for $(\Delta m^2, \sin^2 2\theta)$ in the small mixing angle allowed region, the lower energy *pp* and ^{7}Be neutrinos, which have energies that correspond to the adiabatic regime, will be preferentially depleted, while the higher energy ^{8}B neutrinos have a higher survival probability due to nonadiabatic level jumping. Two neutrino experiments currently under construction, the Sudbury Neutrino Observatory (SNO) and SuperKamiokande, may have the ability to detect the distortion in the ^{8}B neutrino energy spectrum for small angle MSW solutions. For most of the small angle region, SNO should be able to discern the spectral distortion, while it is very unlikely that the minimal shape distortion produced by MSW parameters in the large angle region could be detected.

SNO of course can also measure the ratio of charged current events to neutral current events, which provides an indicator for ν_e oscillations into another active neutrino species. A ratio significantly less than that expected for the SSM (i.e., the ratio of the electron neutrino charged current to neutral currents cross sections [39,40]) would be a strong indication of MSW mixing. However, the neutral current events are signaled by the production of a free neutron, and the background for this process can be problematic.

The improved statistics of SuperKamiokande, which expects to see on the order of 8000 events per year [41], can be used to examine more closely the effects of ν_e regeneration through the Earth (see Sec. IV C). In Fig. 5, we plot the contours for several values of (day-

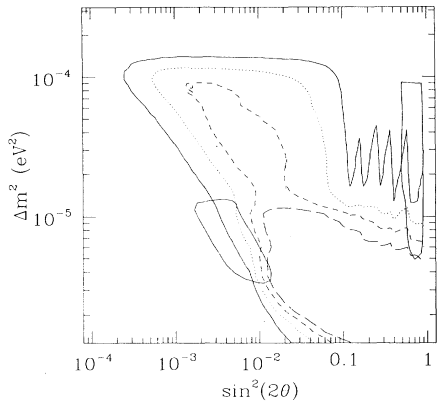

FIG. 5. The allowed region from the fit to the experimental rates, plus the contours of (day-night)/(day+night) rate. The contours are 1% (solid), 5% (dotted), 10% (dashed), and 15% (long-dashed). An average over the night and the year has been assumed for these contours, and the model of the interior of the Earth used was very simplistic.

night)/(day+night), superimposed upon the allowed regions. Recall that our model for calculating the above ratio automatically assumes an average of the year and the entire night and uses a very crude model of the Earth. An analysis using the methods of Sec. IV C on a more realistic model of the Earth could be performed, however Fig. 5 serves to show the potential for narrowing the allowed regions if a positive day-night variation is seen. If SuperKamiokande does find a signal for day-night variation then binning the data vs cos $\delta_{\rm Sun}$ [cf. Eq. (22) with $\delta_{\rm Sun} = (\theta_0 + \pi)/2$] would provide more information than our simple average.

An experiment sensitive to ^{7}Be neutrinos can potentially discriminate between the large and small mixing angle solutions in addition to confirming the depletion of the ^{7}Be flux. The predicted rate for Borexino [42] as a fraction of the standard solar model rate is [43]

$$R_{\rm Borexino} = 0.78P(\nu_e \to \nu_e; {}^7{\rm Be}) + 0.213 \qquad (28)$$

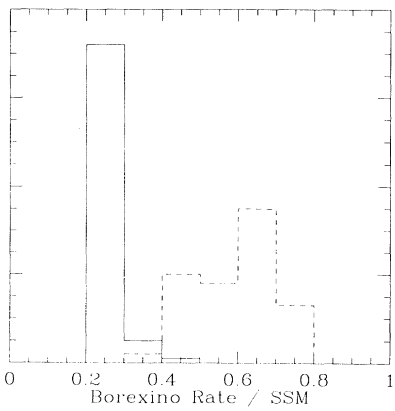

FIG. 6. Predictions for the Borexino event rate as a fraction of the standard solar model value. The histograms show relative frequencies of predicted event rates in the large (dashed) and small (solid) angle regions.

where the 0.213 is absent for oscillations into a sterile neutrino. For the two currently allowed MSW parameter regions, the predicted rates in Borexino are shown in Fig. 6. A Borexino rate of less than 0.3 would provide not only a striking confirmation of the solar neutrino problem, but also indicate the small mixing angle region of the MSW solution, whereas rates between 0.5 and 0.8 would point to the large mixing angle solutions. A detected rate of about 0.35 of the standard solar model would not allow discrimination between the two solutions, but would nonetheless be further evidence in support of new neutrino physics. However note that after 1 yr of running Borexino can at best measure the rate to $\sim 30\%$.

VIII. IMPLICATIONS FOR PARTICLE PHYSICS MODELS

If future experiments confirm the deficit of electron neutrinos indicated by the current data, we would have the first (indirect) evidence of physics beyond the standard model: neutrino masses. Further solar neutrino studies coupled with upcoming neutrino oscillation experiments [44] are the current best hope of seeing neutrino masses in the cosmologically interesting range $\Sigma m_i = 3-30$ eV. (The region of mass-mixing angle space of interest for oscillations which may explain the deficit of atmospheric muon neutrinos can be probed by several proposed long baseline oscillation experiments [45].) The mass-mixing angle parameters implied by the allowed regions shown in Fig. 2, while not indicative of any particular particle physics models for neutrino masses, are consistent with models which incorporate a seesaw mechanism. Many of these models can also accommodate the observed deficit of the ratio of atmospheric ν_μ/ν_e [46] and in some cases also allow for the ν_τ to be cosmological hot dark matter [47] or provide contributions to neutrinoless double β decay at the level of $\bar{m} \sim 1$ eV [48].

There is significant literature in the particle physics community on constructing models which go beyond the standard model of electroweak interactions, and many of these models have interesting implications for neutrino properties. Here we discuss some classes of models which are currently popular and which relate directly to the solar neutrino problem.

Models in which the neutrino mixing angles are similar to the CKM angles in the quark sector [49] now appear to be disfavored by the data. A class of models based on grand unification particle physics models and a seesaw mechanism for neutrino masses [50] give masses and mixings which can lie in the small angle region of Fig. 2 [51,52]. In some cases these models can also incorporate solutions to the atmospheric neutrino deficit, provide the hot dark matter component of currently popular mixed dark matter models (on the order of 1–10 eV in neutrino mass), and even accommodate a Majorana mass of 1–2 eV for neutrinoless double β decay [53]. In these models the masses of the light neutrinos we see are a combination of the Dirac masses of the usual neutrinos plus new right-handed neutrinos ν_R which additionally have Majorana masses. The ν_R are placed in grand unified the-

ory (GUT) gauge group multiplets along with the quarks and leptons and get masses from the same Higgs bosons. This relates the Dirac mass matrices of the neutrinos in these models to those of the quarks and leptons. If further "textures" are assumed for the heavy Majorana mass matrix of the ν_R, one obtains predictions for the masses and mixings of the observed light neutrinos, usually with one free (overall mass) scale and a small number of group theory factors. We note in passing that the presence of (powers of) these group theory factors can significantly alter the naive seesaw predictions.

Other models exist [54–57] which generate masses and mixing angles in the large angle allowed region of 2. Such models can allow for simultaneous solution of the solar and atmospheric neutrinos [56] or link solar neutrinos with double β-decay experiments [55] or both [58].

Some authors have considered a radiative mechanism for the generation of neutrino masses, and found models which can accommodate two of the three neutrino mass solutions (solar neutrinos, atmospheric neutrino deficit, dark matter) [59,60].

Further constraints on models for neutrino masses which invoke oscillations into sterile neutrinos ν_s are obtained by considering big-bang nucleosynthesis [61]. The large angle region is excluded for ν_e-ν_s oscillations based on present observations of the primordial ^{4}He abundance. This also eliminates ν_μ-ν_s solutions to the atmospheric ν_μ deficit. Arguments derived from Supernova considerations can also be used to constrain oscillations [62,63]. For sterile neutrinos the region of mass-mixing angle space restricted by these arguments, while of interest for sterile neutrinos as dark matter candidates, is not relevant for solar neutrino oscillations [63].

IX. CONCLUSIONS

In this paper we have presented an updated analysis of the implications of the four currently operating solar neutrino experiments. Our analysis incorporates a straightforward and comprehensive treatment of the known theoretical statistical uncertainties, which we have outlined in detail. We have given a full account of our methods and assumptions so others can compare with our work.

We find that the current solar neutrino experiments provide a useful constraint on the masses and mixing angles of neutrino in models where neutrino mixing is the resolution of the solar neutrino problem. All the quantifiable errors in established solar models are included in this constraint. Both resonant (MSW) and nonresonant (just-so) neutrino oscillation models are allowed by the data, while the standard solar model and variations of the SSM which suppress the ^{8}B flux are strongly disfavored (at better than the 99.99% level). In considering the implications of these figures, it is important to note that systematic uncertainties remaining in both the solar model calculations and input parameters can have an effect on the properties of the allowed regions, as shown in Fig. 4. Nevertheless, as solar models improve, the consistent statistical analysis we have defined here will continue to gain in significance.

Future experiments have great promise for confirming the solar neutrino problem and firmly establishing the need for neutrino-based solutions. In particular we have examined the potential of SuperKamiokande, SNO, and Borexino to provide further constraints on the masses and mixing angles of neutrinos in such models. If the charged-to-neutral-current ratio measured by SNO indicates the probability of neutrino oscillations, the presence (absence) of spectral distortion will further constrain the mixing parameters to the small (large) angle regions. (While SNO is not capable of distinguishing between large angle oscillations into sterile neutrinos and solar model solutions, such oscillations have already been ruled out by big-bang nucleosynthesis as mentioned above [61].) Borexino also possesses the ability to distinguish between small and large angle MSW regions to some extent. If the large angle solution turns out to be favored, then SuperKamiokande should provide a sensitive probe of the allowed mass and mixing through the measurement of the day-night effect.

Note added in proof. The GALLEX Collaboration mentioned in the text has now been performed successfully. The observed event rate was in good agreement with the predicted event rate with a Cr source inserted in the detector.

ACKNOWLEDGMENTS

We would like to thank J. Bahcall for kindly providing us with the total fluxes from the 1000 solar models of [11], and for helpful discussions. We also thank M. Pinsonneault and N. Hata for useful conversations related to their work. This work was supported in part by the NSF and DOE. M.W. acknowledges the support of the SSC through the TNRLC. L.M.K. and M.W. thank the Institute for Nuclear Theory at the University of Washington for its hospitality and the Department of Energy for partial support during the completion of this work. E.G. was supported by the DOE of the University of Chicago and by the DOE and by NASA through Grant No. NAGW2381 at Fermilab.

[1] M. White, L. M. Krauss, and E. Gates, Phys. Rev. Lett. **70**, 375 (1993).

[2] H. A. Bethe and J. N. Bahcall, Phys. Rev. D **47**, 1298 (1993).

[3] J. N. Bahcall, Phys. Rev. D **44**, 1644 (1991); H. A. Bethe and J. N. Bahcall, *ibid.* **44**, 2962 (1991); J. N. Bahcall and H. A. Bethe, Phys. Rev. Lett. **65**, 2233 (1990); J. N. Bahcall and W. C. Haxton, Phys. Rev. D **40**, 931 (1989).

[4] J. N. Bahcall and W. C. Haxton, Phys. Rev. D **40**, 931 (1989).

[5] S. A. Bludman, D. C. Kennedy, and P. G. Langacker, Phys. Rev. D **45**, 1810 (1992); Nucl. Phys. **B374**, 373 (1992); **B373**, 498 (1992); in *Neutrino '92*, Proceedings of the XVth International Conference on Neutrino Physics and Astrophysics, Granada, Spain, 1992, edited by A. Morales [Nucl. Phys. B (Proc. Suppl.) **31**, 156 (1993)].

[6] X. Shi, D. N. Schramm, and J. N. Bahcall, Phys. Rev. Lett. **69**, 717 (1992); X. Shi and D. N. Schramm, Phys. Lett. B **283**, 305 (1992); X. Shi, D. N. Schramm, and D.

S. P. Dearborn, Phys. Rev. D **50**, 2414 (1994).
[7] P. I. Krastev and S. T. Petcov, Phys. Lett. B **299**, 99 (1993).
[8] W. Kwong and S. P. Rosen, Phys. Rev. Lett. **73**, 369 (1994).
[9] S. P. Mikheyev and A. Yu. Smirnov, Yad. Fiz. **42**, 1441 (1985) [Sov. J. Nucl. Phys. **42**, 913 (1985)] Nuovo Cimento 9C, 17 (1986); L. Wolfenstein, Phys. Rev. D **17**, 2369 (1987); **20**, 2634 (1989).
[10] N. Hata and P. Langacker, Phys. Rev. D **49**, 632 (1994).
[11] J. N. Bahcall and R. K. Ulrich, Rev. Mod. Phys. **60**, 297 (1988).
[12] J. N. Bahcall, *Neutrino Astrophysics* (Cambridge University Press, Cambridge, England, 1989).
[13] S. A. Bludman, N. Hata, D. C. Kennedy, and P. G. Langacker, Phys. Rev. D **47**, 2220 (1993).
[14] J. Mathews and R. L. Walker, *Methods of Mathematical Physics*, 2nd ed. (Addison-Wesley, Reading, MA, 1970); T. J. Loredo, in *Statistical Challenges in Modern Astronomy*, edited by E. D. Feigelson and G. J. Babu (Springer-Verlag, New York, 1992).
[15] L. M. Krauss, E. Gates, and M. White, Phys. Lett. B **299**, 94 (1993).
[16] J. N. Bahcall and M. H. Pinsonneault, Rev. Mod. Phys. **64**, 885 (1992).
[17] V. Gribov and B. Pontecorvo, Phys. Lett. **28B**, 493 (1969); S. M. Bilenky and B. Pontecorvo, Phys. Rep. **41**, 225 (1978); S. M. Bilenky and S. T. Petcov, Rev. Mod. Phys. **59**, 671 (1987).
[18] P. I. Krastev and S. T. Petcov, Phys. Rev. Lett. **72**, 1960 (1994).
[19] N. Hata, U. Penn. Report No. UPR-0605T, 1994 (unpublished).
[20] R. Davis, Jr., in *Proceedings of the Seventh Workshop on Grand Unification*, Toyama, 1986, edited by J. Arafune (World Scientific, Singapore, 1986), p. 237; in *Frontiers of Neutrino Astrophysics*, Tokyo, 1993, edited by Y. Suzuki and K. Nakamura (Universal Academy Press, Tokyo, Japan, 1993), p. 47; K. Lande, talk presented at "XVI International Conference on Neutrino Physics and Astrophysics," Eilat, Israel, 1994 (unpublished).
[21] K. Hirata *et al.*, Phys. Rev. Lett. **63**, 16 (1989); **65**, 1297 (1990); **65**, 1301 (1990); **66**, 9 (1991); A. Suzuki, in *Proceedings of the ICEPP Symposium "From LEP to the Planck World,"* Tokyo, Japan, 1992, edited by K. Kawagal and T. Kobayashi (VT-ICEPP Report No. 93-12, Tokyo, 1993).
[22] A. I. Abazov *et al.*, Phys. Rev. Lett. **67**, 3332 (1991); in *Neutrino 90*, Proceedings of the 14th International Conference on Neutrino Physics and Astrophysics, Geneva, Switzerland, edited by J. Panam and K. Winter [Nucl. Phys. B (Proc. Suppl.) **19**, 84 (1991)].
[23] P. Anselman *et al.*, Phys. Lett. B **285**, 376 (1992); **285**, 390 (1992); **314**, 445 (1993).
[24] P. I. Krastev and S. T. Petcov, Phys. Lett. B **207**, 64 (1988).
[25] W. C. Haxton, Phys. Rev. D **35**, 2352 (1987); S. J. Parke, Phys. Rev. Lett. **57**, 1275 (1986); P. Pizzochero, Phys. Rev. D **36**, 2293 (1987); T. K. Kuo and J. Pantaleone, Rev. Mod. Phys. **61**, 937 (1989).
[26] E. D. Carlson, Phys. Rev. D **34**, 1454 (1986); J. Boucher, M. Cribier, W. Hampel, J. Rich, M. Spiro, and D. Vignaud, Z. Phys. C **32**, 499 (1986).
[27] N. Hata and P. Langacker, Phys. Rev. D **48**, 2937 (1993).
[28] A. J. Baltz and J. Weneser, Phys. Rev. D **35**, 528 (1987); **37**, 3364 (1988).
[29] A. M. Dziewonski, A. L. Hales, and E. R. Lapwood, Phys. Earth Planet. Inter. **10**, 12 (1975); F. D. Stacey, *Physics of the Earth*, 2nd ed. (Wiley, New York, 1985).
[30] E. Gates, L. M. Krauss, and M. White, Phys. Rev. D **46**, 1263 (1992).
[31] K. Hirata *et al.*, Phys. Rev. D **44**, 2241 (1991); M. Nakahata, Ph.D. thesis.
[32] See, for example, E. L. Lehmann, *Testing Statistical Hypotheses* (Wiley-Interscience, New York, 1986); A. C. S. Readhead and C. R. Lawrence, Annu. Rev. Astron. Astrophys. **30**, 653 (1992); A. C. S. Readhead *et al.*, Astrophys. J. **346**, 566, Sec. VIII (1989); Particle Data Group, K. Hikasa *et al.*, Phys. Rev. D **45**, S1 (1992); C. Howson and P. Urbach, Nature (London) **350**, 371 (1991); J. Skilling, *ibid.* **353**, 707 (1991); A. W. F. Edwards, *ibid.* **352**, 386 (1991).
[33] J. O. Berger, *Statistical Decision Theory and Bayesian Analysis*, 2nd ed. (Springer-Verlag, Berlin, 1985).
[34] A. W. F. Edwards, *Likelihood* (Cambridge, University Press, Cambridge, England, 1984).
[35] R. W. Kavanagh *et al.*, Bull. Am. Phys. Soc. **14**, 1209 (1969).
[36] B. W. Filippone *et al.*, Phys. Rev. C **28**, 2222 (1983).
[37] C. Proffitt, talk given at "Solar Modelling Workshop," INT, Seattle, 1994 (unpublished).
[38] M. Pinsonneault (private communication).
[39] G. T. Ewan *et al.*, in *Frontiers of Neutrino Astrophysics*, edited by Y. Suzuki and K. Nakamura (Universal Academy Press, Tokyo, Japan, 1993), p. 147.
[40] J. N. Bahcall, K. Kubodera, and S. Nozawa, Phys. Rev. D **38**, 1030 (1988).
[41] M. Takita, in *Frontiers of Neutrino Astrophysics* [20], p. 135.
[42] R. S. Raghavan *et al.*, Phys. Rev. D **44**, 3786 (1991).
[43] J. M. Gelb, W. Kwong, and S. P. Rosen, Phys. Rev. Lett. **69**, 1864 (1992); W. Kwong and S. P. Rosen, *ibid.* **68**, 748 (1992).
[44] CHORUS Collaboration, N. Armenise *et al.*, Report No. CERN-SPSC/90-42, 1990 (unpublished); E803 Collaboration, K. Kodama *et al.*, FNAL proposal, 1993 (unpublished); NOMAD Collaboration, P. Astier *et al.*, Report No. CERN-SPSLC/92-21, 1992 (unpublished).
[45] S. Parke, in *Perspectives in Neutrinos, Atomic Physics and Gravitation*, Proceedings of 1993 Moriond Meeting, edited by J. Tran Thanh Van *et al.* (Editions Frontières, Gif-sur-Yvette, France, 1993).
[46] K. S. Hirata, *et al.*, Phys. Lett. B **280**, 146 (1992); R. Becker-Szendy *et al.*, Phys. Rev. D **46**, 3720 (1992); P. J. Litchfield, in International Europhysics Conference on High Energy Physics, Marseille, France, 1993 (unpublished).
[47] Q. Shafi and F. Stecker, Phys. Rev. Lett. **53**, 1292 (1984); D. Tommasini, Report No. FTUV/94-1 (unpublished).
[48] A. Piepke, in *Proceedings of the International Europhysics Conference on High Energy Physics*, Marseille, France, edited by J. Carr and M. Perottet (Editions Frontières, Gif-Sur-Yvette, France, 1993); E. Garcia, in *TAUP 93*, Proceedings of the Workshop, Gran Sasso, Italy, 1993, edited by C. Arpesella *et al.* [Nucl. Phys. B (Proc. Suppl.) **35** (1994)].
[49] P. Langacker and M. Luo, Phys. Rev. D **44**, 817 (1991); P. Langacker *et al.*, Nucl. Phys. **B282**, 589 (1987).

[50] M. Gell-Mann, P. Ramond, and R. Slansky, in *Supergravity*, Proceedings of the Workshop, Stony Brook, New York, 1974, edited by P. van Nieuwenhuizen and D. Freedman (North-Holland, Amsterdam, 1979), p. 315.
[51] J. Harvey, D. Reiss, and P. Raymond, Phys. Lett. **92B**, 309 (1980); Nucl. Phys. **B199**, 223 (1982).
[52] K. S. Babu and Q. Shafi, Phys. Rev. D **47**, 5004 (1993); Phys. Lett. B **194**, 235 (1992); S. Dimopoulos, L. J. Hall, and S. Raby, Phys. Rev. D **47**, 3697 (1993); K. S. Babu and R. N. Mohapatra, Phys. Rev. Lett. **70**, 2845 (1993); G. Anderson *et al.*, Phys. Rev. D **49**, 3660 (1994); C. H. Albright and S. Nandi, Phys. Rev. Lett. **73**, 930 (1994); E. Papageorgiu, report (unpublished); D. Lee and R. N. Mohapatra, Phys. Lett. B **329**, 463 (1994).
[53] D. O. Caldwell and R. N. Mohapatra, Phys. Rev. D **48**, 3259 (1993); D. O. Caldwell and R. N. Mohapatra, *ibid.* **50**, 3477 (1994).
[54] A. Smirnov, Phys. Rev. D **48**, 3264 (1993).
[55] S. T. Petcov and A. Yu Smirnov, Phys. Lett. B **322**, 109 (1994).
[56] C. W. Kim and J. A. Lee, Report No. JHU-TIPAC-930023 (unpublished).
[57] L. Lavoura, Phys. Rev. D **48**, 5440 (1993).
[58] C. P. Burgess, Phys. Rev. D **48**, 4326 (1993).
[59] H. A. Bethe, Phys. Rev. Lett. **56**, 1305 (1986); S. P. Rosen and J. M. Gelb, Phys. Rev. D **34**, 969 (1986); E. W. Kolb, M. S. Turner, and T. P. Walker, Phys. Lett. B **175**, 478 (1986).
[60] A. Y. Smirnov and Z. Tau, Nucl. Phys. **B426**, 415 (1994), and references therein.
[61] X. Shi, D. N. Schramm, and B. D. Fields, Phys. Rev. D **48**, 2563 (1993).
[62] Y.-Z Qian *et al.*, Phys. Rev. Lett. **71**, 1965 (1993).
[63] X. Shi and G. Sigl, Phys. Lett. B **323**, 360 (1994).

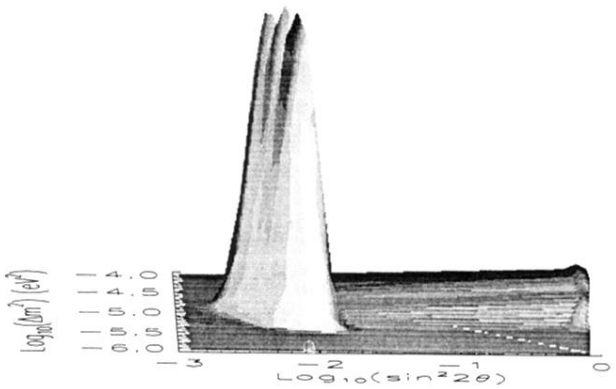

FIG. 3. Likelihood function $\mathcal{L}(\log \Delta m^2, \log \sin^2 2\theta)$ for the combined Homestake-Kamiokande-Gallium data.